J Fluoresc (2013) 23:881–888
DOI 10.1007/s10895-013-1194-x

ORIGINAL PAPER

Detection of Target Proteins by Fluorescence Anisotropy

Lin Wang · Brendan Clifford · Lacey Graybeal · Luke Tolley · Matthew E. McCarroll

Received: 13 September 2012 / Accepted: 24 February 2013 / Published online: 11 April 2013

Abstract Understanding molecular interactions is critical to understanding most biological mechanisms of cells and organisms. In the case of small molecule–protein interactions, many molecules have significant biological activity through interactions with unknown target proteins and by unknown modes of action. Identifying these target proteins is of significant importance and ongoing work in our laboratories is developing a technique termed Dynamic Isoelectric Anisotropy Binding Ligand Assay (DIABLA) to meet this need. Work presented in this manuscript aims to characterize the fundamental parameters affecting the use of fluorescence anisotropy to detect target proteins for a given ligand. Emphasis is placed on evaluating the use of fluorescence anisotropy as a detection mechanism, including optimization factors that affect the protein detection limit. Effects of ligand concentration, pH, and nonspecific binding are also examined.

Keywords Protein · Ligand · Fluorescence anisotropy · Modeling

Many molecules that are known to play important roles in modulating or affecting cellular function do so with unknown modes of action, examples of which include pharmaceutical compounds, environmental pollutants, RNA, and peptides. With some notable exceptions, modes of action all involve the biologically active species (ligands) binding to proteins (often unknown) serving various biological functions. Identifying these target proteins can greatly increase our understanding of the mode of action in these systems. In the area of drug discovery, finding a particular protein target for a specific drug molecule stands as the ultimate goal with respect to drug design [1–3]. To date, studies of ligand–protein interactions have been carried out by various techniques [4, 5]. Some of the most common used techniques are affinity chromatography, protein arrays, surface plasmon resonance and fluorescence energy transfer, etc. Affinity chromatography, as an effective separating method [6], has been successfully applied to isolating ligands from a compound mixture even for a very weak binder, as low as 100 μM to 1 mM [7]. Protein arrays have been widely used as microarrays of protein domains to obtain equilibrium dissociation constants for both high-affinity and low-affinity binding ligands [8]. Surface plasmon resonance (SPR) is a well-demonstrated technique for the detection of proteins interacting with small molecules, allowing the chip-based determination of binding constants [9, 10]. Fluorescence resonance energy transfer (FRET) has also been applied to detect the presence of ligands and in some cases single-molecule detection can be achieved [11]. There are other novel methods that have been reported recently. In 2009, Zhusheng Ji et al. introduced a saturation transfer difference NMR that was able to measure the dissociation constant of a specific ligand–protein binding [12]. In another study, Osborne et al. reported an investigation on the dynamics of a ligand–protein system by single-molecule orientational imaging [13]. Mass spectrometry, as well as capillary electrophoresis, have also been used for this area of study [14–16]. Generally, most studies are performed on one model ligand and one related model protein. Notably, the analysis of one ligand in a complex protein mixture and the detection of unknown protein targets remain a challenging, if not elusive task.

To address this challenge, our groups are developing a new technique termed dynamic isoelectric anisotropy binding ligand assay (DIABLA) that is designed to meet this

L. Wang · B. Clifford · L. Graybeal · L. Tolley · M. E. McCarroll (✉)
Department of Chemistry and Biochemistry, Southern Illinois University, Carbondale, IL 62901, USA
e-mail: mmccarroll@chem.siu.edu

need. This technique combines the recently developed technique of dynamic isoelectric focusing (DIEF) and fluorescence anisotropy to identify protein targets for a given ligand molecule [17, 18]. Dynamic IEF is a modification of capillary IEF where additional electrodes are used within the capillary to dynamically tune the pH gradient, thus imparting an ability to move focused protein bands to a sampling point in the capillary. The work detailed here represents recent efforts in our laboratory to characterize fundamental and practical aspects of using fluorescence anisotropy as a method to detect the presence of a target protein using both intrinsic fluorescence and fluorescently tagged ligands.

Fluorescence anisotropy is a spectroscopic method based on polarization that has been widely used to study molecular mobility and molecular interactions, particularly in biological systems [3, 19–23]. As representation of the degree of polarization, anisotropy is typically used as a measure of the polarization due to the comparatively simple equations relating depolarization to molecular rotation. The dependence of fluorescence anisotropy on molecular rotation can be described quantitatively with the well know Perrin equation,

$$\frac{r_0}{r} = 1 + \frac{\tau}{\phi} = 1 + \frac{\tau RT}{\eta V}, \quad (1)$$

where r is the measured aniotropy, r_0 is the intrinsic anisotropy, ϕ is the rotational correlation time, τ is the fluorescence lifetime, R is the gas constant, T is the temperature in K, and V is the volume of the rotating unit. As predicted by Perrin equation, free ligand molecules typically have very fast rotational correlation times and display a very small measured anisotropy for typical fluorescence lifetime. On the other hand, ligands that bind to the protein possess a slower rotational correlation time that leads to a corresponding higher measured anisotropy value.

In the case of protein–ligand (host–guest) interactions, an analyte generally exists in one of two forms, the bound complex or the free species. Based on the additive properties of polarization, the total anisotropy for the binding system is a weighted average of the anisotropy values of the bound species and free analytes as shown in Eq. 2,

$$r_{avg} = f_{bound} r_{bound} + f_{free} r_{free} \quad (2)$$

where f_{bound} and f_{free} are the fraction of fluorescence intensity of bound and free species, r_{bound} and r_{free} are the anisotropy values of bound and free species, respectively. Therefore, the measured anisotropy value can be used as an indicator of ligand–protein binding, which depends on the concentration of the ligand and protein, as well as binding constant.

Fluorescence anisotropy has long been used as an effective tool for investigating protein–ligand interactions. In the work K. Callaway et al. published in 2005, fluorescence anisotropy binding studies were focused on understanding the effects of protein ligands on ERK2 distribution [24]. In another report, Thomas Hey and colleagues employed fluorescence anisotropy measurements to investigate proteins XPA and RPA binding with damaged DNA [23]. An enhanced fluorescence anisotropy assay was newly developed to simultaneously detect two protein biomarkers human cardiac troponin I and troponin T [25]. These works are modern examples that fluorescence anisotropy is highly capable in the task of revealing protein–ligand and protein–protein interactions. Although most work thus far emphasizes the practicalities of fluorescence anisotropy on either thermodynamic analysis or kinetic studies of protein–ligand interactions, our work detailed in this paper focuses on a detailed investigation and optimization for using fluorescence anisotropy to detect ligand–protein interactions, using anisotropy measurements as a method to determine the presence of protein targets, as is particularly relevant in developing the DIABLA technique.

Materials and Methods

Chemicals and Materials The structures of the ligands that were used are shown in Fig. 1. Cyclooxygenase-1 (COX-1) ≥95 % was obtained from Sigma-Aldrich Co. (St. Louis, MO). Ibuprofen 99 % and Tris buffer pH8.0 (Ultrapure) were obtained from Fisher Scientific (Fair Lawn, NJ). Naproxen 99.3 % was purchased from MP Biomedicals, LLC. Biotin (fluorescein conjugated) and streptavidin were obtained from EMD Chemicals Inc. (Darmstadt, Germany). A polar screen progesterone receptor competitor assay kit was obtained from Invitrogen Co. (Carlsbad, CA). (This kit was originally designed for competitor assay. Here it is used as a direct binding assay.). All analytes in COX-1 systems were prepared using Tris buffer (pH8.0). Water

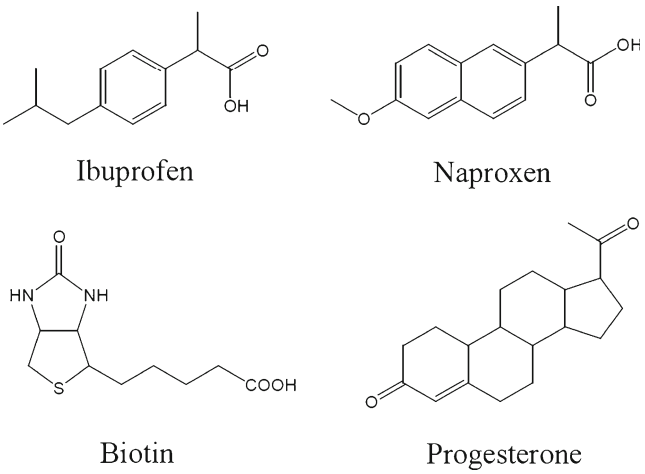

Fig. 1 Structures of the ligands used in the binding study

used in all experiments was purified by a Milli-Q system (Millipore Inc., Milford, MA) to a resistance of at least 18 MΩ. 600 μL and 100 μL quartz cuvettes were used and purchased from Starna Cells Inc. (Atascadero, CA).

Sample Preparation All ligands used in this study have either intrinsic fluorescence (e.g. ibuprofen, naproxen) or have been fluorescecently labeled (e.g. progesterone and biotin have been tagged with fluorescein). In the COX-1 systems, the solutions containing the ligand and COX-1, respectively, were prepared using Tris buffer, to obtain a pH of 8.0, which has been claimed by the manufacturer to represent conditions that retain binding activity. For each system, a series of solutions were made with constant ligand concentration and varying protein concentrations. All solutions were mixed by gently pipetting and then allowed to equilibrate for at least 1 h prior to measurement.

Fluorescence Measurements Steady-state fluorescence measurements were performed using modular spectrofluorometers from either Photon Technology International Inc. or Horiba Jobin Yvon Inc. using a xenon arc lamp for excitation and double excitation and emission monochromators for wavelength discrimination. Excitation and emission monochromator slits were adjusted for spectral band-passes ranging from 2 nm to 10 nm depending on the fluorescence intensity. Fluorescence anisotropy measurements were carried out at a temperature of 25 °C controlled by a thermocirculator and used automated Glann-Thompson polarizers with a T-optics configuration and G-factor correction for any instrumental polarization bias. Photomultiplier tubes were used for detection in the single-photon counting mode. A 30–60 s integration time was used for each run, and at least three replicate measurements were recorded.

Results and Discussion

Binding Curve Modeling For ligand–protein interaction systems, a binding curve is the trend of increasing anisotropy as a function of increased total protein concentration. To predict the binding curve of a given system, we consider a solution containing the ligand (*L*), protein (*P*), and the complex (*PL*) with an association equilibrium given in Eq. 3.

$$P + L \xleftrightarrow{K_b} PL \tag{3}$$

The binding constant (K_b) and dissociation constant (K_d) for this system can then be expressed as Eq. 4,

$$K_b = \frac{[PL]}{[P][L]} = \frac{1}{K_d}, \tag{4}$$

Here, [*P*] and [*L*] represent the concentration of the free protein and ligand, respectively, and [*PL*] is the concentration of the complex. Combining Eqs. 3 and 4 allows evaluation of the fraction of the bound species with concentration of ligand ([*L*]), protein concentration ([*P*]), as given by Eqs. 5 and 6.

$$f_b = \frac{[PL]}{[L] + [PL]} \tag{5}$$

$$f_b = \frac{[P]}{[P] + K_d} \tag{6}$$

Because all the ligands are either bound or free species, as shown in Eq. 7.

$$f_b + f_f = 1 \tag{7}$$

Therefore we can express f_f as is shown in Eq. 8.

$$f_f = \frac{K_d}{[P] + K_d} \tag{8}$$

The concentration of the bound protein is given by the total protein concentration $[P]_t$ minus the free protein [*P*]. In the 1:1 binding system, the concentration of bound protein equals to the concentration of bound ligand. Then the concentration of free ligand will be the concentration of bound ligand subtracted from the total ligand concentration as in Eq. 9.

$$[L] = [L]_t - [PL] = [L]_t - [P]_t + [P] \tag{9}$$

Analysis Eqs. 4 and 9, allows one to arrive at K_d as a function of total ligand and protein concentration as well as free protein concentration shown in Eq. 10,

$$K_d = \frac{[P]\left([L]_t - [P]_t + [P]\right)}{[P]_t - [P]} \tag{10}$$

Solving Eq. 10 for [*P*] can be expressed as shown in Eq. 11.

$$[P] = \frac{1}{2}\left(-K_d - [L]_t + [P]_t + \sqrt{\left(K_d + [L]_t - [P]_t\right)^2 + 4K_d[P]_t}\right) \tag{11}$$

The measured steady-state anisotropy value can then be expressed with respect to the dissociation constant, the anisotropy of the bound and free ligand, and the concentration of free protein as indicated in Eq. 12.

$$r_{avg} = \frac{K_d \times r_f + [P] \times r_b}{[P] + K_d} \tag{12}$$

Using appropriate values for the anisotropy of free and bound ligands and the total ligand concentration, a

prediction of anisotropy values for various total protein concentrations and dissociation constants can be made, as shown in Fig. 2. The 3D model (Fig. 2a) requires evaluation of two variables, the dissociation constant and the total protein concentration. With varied magnitude of dissociation constant, binding curves were generated showing an increasing trend, as expected. Overall, as the total protein concentration is increased, the equilibrium is pushed toward the bound form, resulting in an increasing anisotropy value. Figure 2b illustrates this effect by showing the calculated binding curves for 3 different K_d values. The increasing trend of the binding curve with various K_d shows significant difference. The smaller the K_d, the faster the increase is.

To experimentally evaluate the correlation between the anisotropy and total protein concentration and use anisotropy to detect target proteins, various ligand–protein systems have been investigated, including the naproxen-COX-1 system and ibuprofen-COX-1 system, as examples for intrinsic fluorescent ligand; progesterone–progesterone receptor system and the biotin-streptavidin system, as examples for fluorescent labeled ligand. Various other factors can have influence on the shape of binding curve have also been investigated, such as ligand concentration, solution pH, and non-specific binding.

Naproxen-COX-1 System Naproxen, a well-known drug used to relieve pain and reduce fever, originally marketed as Naprosyn in 1976. It is classified as a nonsteroidal anti-inflammatory drug (NSAID) based on the ability to inhibit the activity of cycoloxygenase (COX). The binding of naproxen and COX-1 was investigated in this study using the intrinsic fluorescence of naproxen. The use of intrinsic fluorescence in binding studies is advantageous because it does not introduce potential artifacts as a result of tagging with an extrinsic probe. Measured quantum yield for naproxen is around 0.23, and we were able to largely avoid direct protein fluorescence by excitation at 330 nm and monitoring the emission at 360 nm, as shown in Fig. 3. Figure 4 shows the smooth increase in anisotropy that was observed at low protein concentrations with constant naproxen concentration at 1 μM, suggesting a detectable concentration level at 0.27 μM in this system. While there are various accepted methods of indicating a detection limit, here we take a value three times the standard deviation of the background measurement ([P]=0) indicates the ability to identify ligand presence at 0.27 μM. Curve fitting for the experimental data using the developed model (Mathematica, Wolfram) resulted in a K_d value 4.54 μM with a standard error 1.98 μM. Comparable literature values for dissociation constants of the naproxen-COX-1 system could not be identified.

Ibuprofen-COX-1 System Ibuprofen is another commonly used NSAID that is a non-selective COX-inhibitor, first became available in 1969. The intrinsic fluorescence of ibuprofen is also used here for anisotropy measurement of the system. However, in the case of ibuprofen it represents a significant challenge due to the weakness and spectral region of the fluorescence signal. Measured excitation and emission maxima for ibuprofen were 290 nm and 358 nm, respectively and the quantum yield was determined to be 0.008. In this region of the spectrum protein fluorescence must be considered, due to the fact that tryptophan residues generally absorb around 290 nm and emit around 350 nm. Direct excitation at 290 nm would lead to excitation of both ibuprofen and the COX-1 protein and would likely cause difficulty in the anisotropy measurement. For this reason, an excitation wavelength of 260 nm was used, sacrificing some signal intensity for avoidance of significant protein fluorescence (See Fig. 5). Figure 6 shows the measured binding curve for the ibuprofen system, where the ligand concentration was fixed at 25 nM and the protein concentration was varied from 1 to 70 nM. Estimated detection limit for this system is at a concentration of approximately 10 nM. Figure 6 also shows the fit of experimental data using the developed model, resulting in a estimated dissociation constant of 41 nM with a standard error 68nM which falls in the reported range of 50 nM-100 nM [26, 27]. The error bars

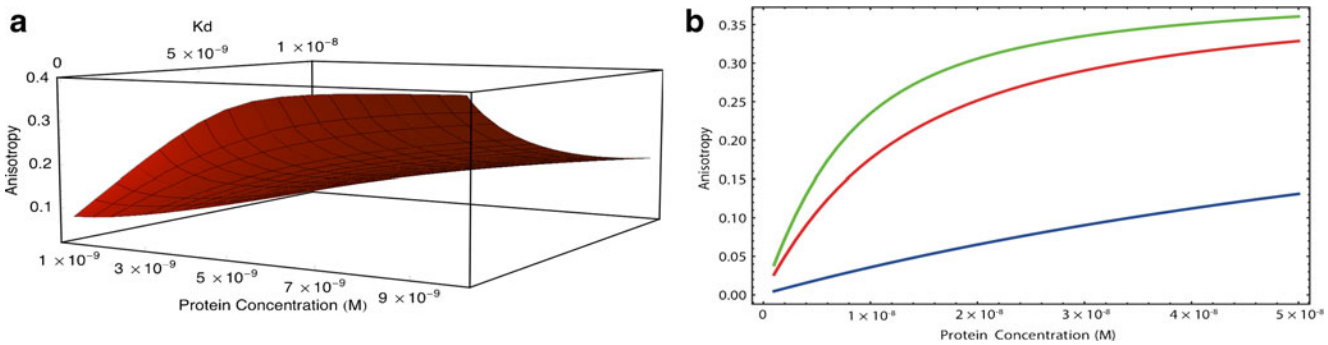

Fig. 2 Binding curve modeling: **a** Predicted anisotropy of ligand as a function of protein concentration as well as K_d (Wolfram Mathematica). **b** Predicted anisotropy of ligand as a function of protein concentration with K_d values fixed at 5 nM (*Green*), 10 nM (*Red*), and 100 nM (*Blue*)

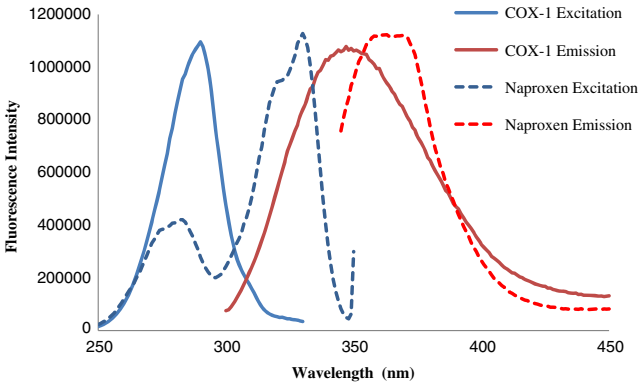

Fig. 3 Excitation and emission spectra of naproxen and COX-1 protein

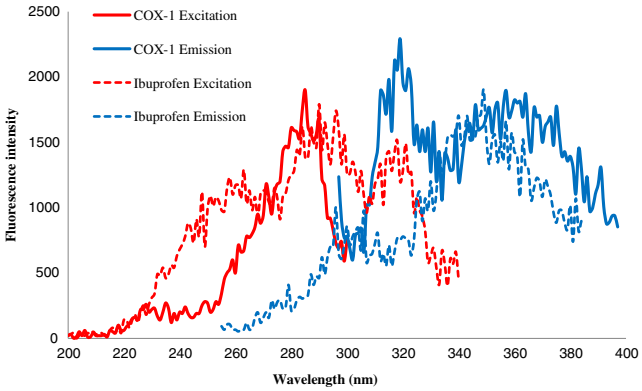

Fig. 5 Excitation and emission spectra of ibuprofen and COX-1 protein

are larger in this system, likely due to the very low quantum yield of ibuprofen.

In order to evaluate the use of extrinsic probes, which typically have better quantum yields, for monitoring direct binding interactions we have chosen to examine two systems where the ligands are labeled with fluorescein. Specifically, labeled progesterone and biotin are examined with their corresponding protein targets.

Progesterone–Progesterone Receptor System Progesterone receptor, known as an intracellular steroid receptor, binds specifically to progesterone, a C-21 steroid hormone that plays a role in breast cancer development and progression. In this work, a polar screen progesterone receptor competitor assay kit was purchased from Invitrogen with progesterone labeled with fluorescein. The K_d value of fluorescently-tagged progesterone ligand (PL) with human progesterone receptor (PR) is reported by the manufacturer to be ~10 nM. In the ligand–protein mixture examined, the concentration of PL was held constant at 2 nM while the concentration of PR protein was increased from 1 nM to 80 nM. All the solutions were first diluted using the PR screening buffer that contained protein stabilizing agents and glycerol (from kit), and then mixed by gently pipetting. The measurements were carried out in a 100 μl quartz cell with a 4 mm pathlength. Figure 7 shows the binding curve, as indicated by the anisotropy value as a function of total progesterone receptor concentration. As expected, an increase in the total concentration of the receptor resulted in an increase in the observed anisotropy. In contrast, the mixture of progesterone ligand and BSA shows a relatively flat binding curve, indicating minimal non-specific interactions.

The effect of ligand concentration was also examined. Figure 7 (inset) shows that variation of the progesterone concentrations (2 nM & 4 nM) results in a shift in the binding curve with a corresponding change in the detection limit from about 10 nM to 20 nM. Fitting of the developed model to experimental data indicates a K_d value of 9.22 nM (standard error=2.1nM), which is very close to the reproted value 10 nM for this labeled ligand (Fig. 7). Labeling of fluorescein to progesterone does not appear to influence its interaction with progesterone receptor and the high quantum yield leads to an accurate result.

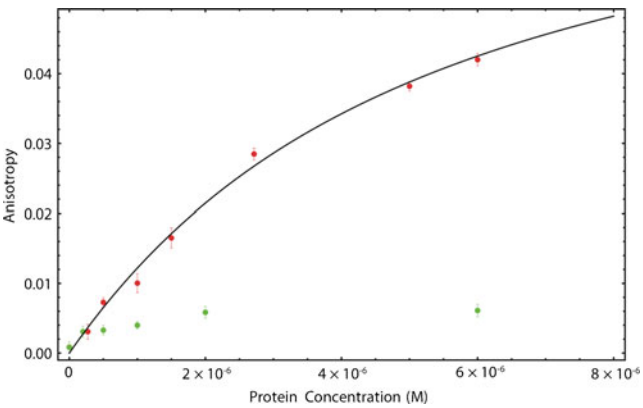

Fig. 4 Binding curve of naproxen-COX-1 based on experimental data (*red dot*) with comparison to nonspecific binding of naproxen-BSA (*Green dot*)

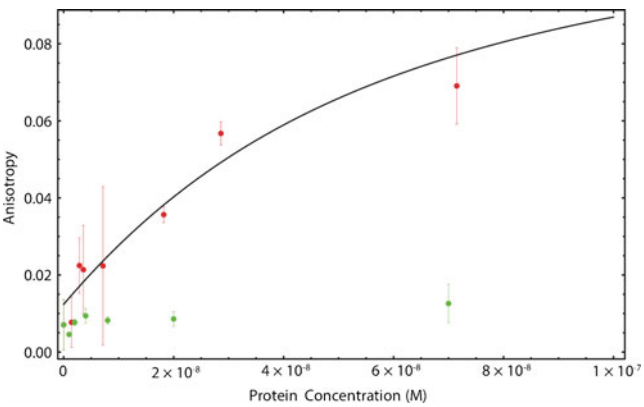

Fig. 6 Binding curve of ibuprofen-COX-1 based on experimental data (*red*) with comparison to nonspecific binding of ibuprofen-BSA (*green*)

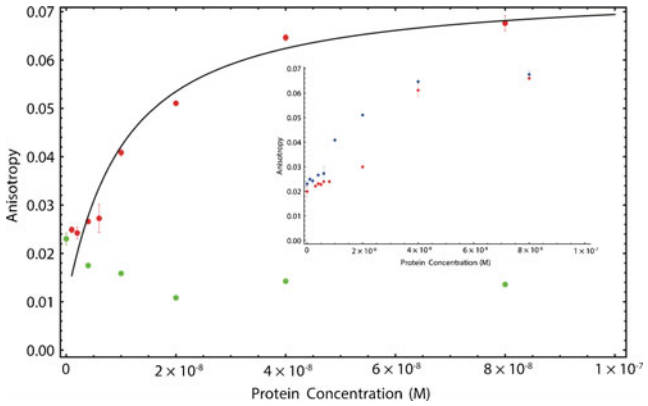

Fig. 7 Binding curve of progesterone-progesterone receptor based on experimental data (*red*) and nonspecific binding of progesterone-BSA (*Green dot*). Inset shows binding curve with different progesterone ligand concentrations (*Blue* 2 nM & Red 4 nM)

Biotin-Streptavidin System Biotin-Streptavidin is commonly used as a model system for binding studies because of the very high affinity ($K_d = 10^{-15}$ M). As a tetrameric protein, each straptavidin molecule binds 4 molecules of biotin. The biotin used in this system was fluorescein conjugated, which allowed for excitation at 494 nm and emission at 521 nm in the fluorescence anisotropy measurements. In this system, the anisotropy was measured for a series of solutions with a constant biotin ligand concentration of 0.85 μM and streptavidin concentrations ranging from 8.5 nM to 0.85 μM. To evaluate non-specific interactions, biotin-BSA binding was analyzed over the same concentration range. Figure 8a shows the comparison of the binding of biotin-streptavidin complex and biotin-BSA complex, where an increase in anisotropy from 0.04 to 0.25 was observed. The anisotropy of biotin-BSA did not increase. Interestingly, the measured binding curve of the biotin-streptavidin system was not as smooth, rather it shows what appears to be undulating structure. The structure to the curve may be related to the fact that the binding of biotin-streptavidin is 4 to 1 ratio and would have a more complex overall equilibrium due to the effects of the multiple binding sites.

The concentration of biotin was varied at concentrations of 0.425 μM (blue), 0.625 μM (red), 0.85 μM (green), and 1.7 μM (purple), as shown in Fig. 8b. Similar to what was observed in the progesterone–progesterone receptor system, the binding curve for biotin-streptavidin system shifts as the concentration

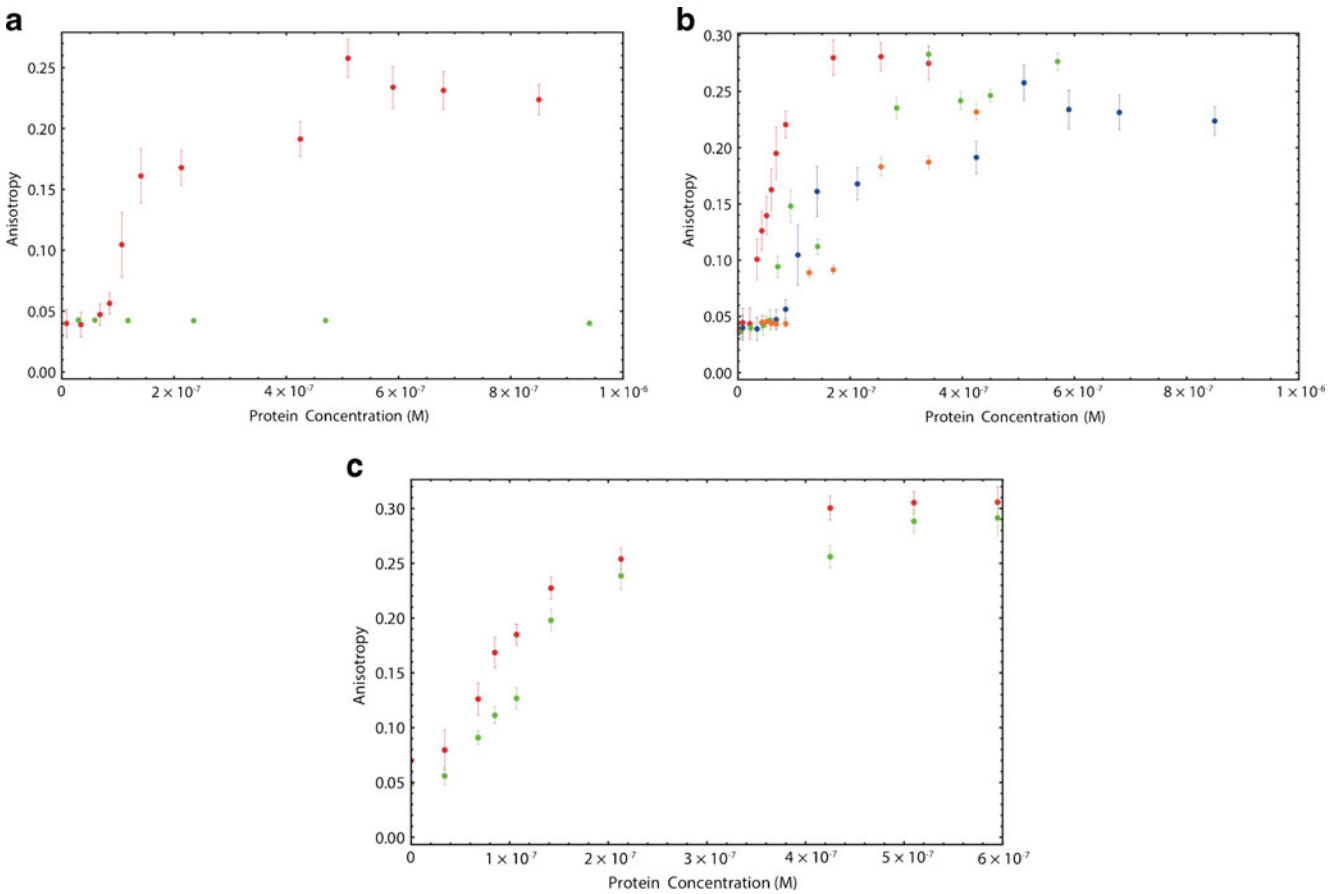

Fig. 8 Binding curves for **a** biotin-streptavidin (*red*) and biotin-BSA (*green*), **b** biotin-streptavidin with various biotin ligand concentrations, and **c** biotin-streptavidin at pH7.0 (*Green*) and 5.5 (*Red*)

of the biotin changes (Fig. 8b). As expected, the lower ligand concentrations resulted in a decrease in the detection limit of the protein, with the lowest observed at a value of 40 nM.

Since the primary drive for this research is to determine fundamental parameters affecting the detection of ligand–protein binding for DIABLA technique, the effect of pH must also be considered. Proteins may focus at pH values that differ from physiological pH. Effects of pH are evaluated on the biotin-streptavidin system since it is a well-studied system with an excellent ligand fluorescence quantum yield. In the case of streptavidin, the binding curve was examined at pH values of 7.0 and 5.5, corresponding to physiological pH and the pI value of streptavidin, respectively. The biotin concentration was held constant at 0.425 μM. As can be seen in Fig. 8c, the change in pH does result in a change in the binding curve, but the ability to detect the protein is not significantly impaired. Fitting to the model was not carried out in the case of the biotin-streptavidin system due to the difficulties in modeling the complex equilibrium associate with the multiple binding sites.

Conclusion

In the present work we have described a detailed approach that uses fluorescence anisotropy to investigate interactions between the ligands and target proteins both through modeling and experimental measurement. Several factors have been taken into consideration for various systems, including ligand concentration, pH, etc. The effects of non-specific binding was also investigated. This work has shown that for a specific ligand–protein binding anisotropy increases significantly as we expected in the modeled binding curve. By varying the concentration of ligand as well as pH value, the detection limit of some systems can be as low as the nanomolar regime. The detection limit depends not only on the dissociation(association) constant of the system but also the quantum yield of the ligand. Excellent sensitivity and selectivity makes this method a good one to discover the target protein in the mixture for a specific drug ligand. In some cases, the fluorescence spectrum of the ligand and of the protein overlaps which lead to the loss of accuracy of the measurement. In order to solve this problem, we choose to excite the ligand at a different wavelength away from the overlapping area, which minimizes excitation of the protein but still provides suitable ligand fluorescence. Ongoing and future studies will examine mixtures of proteins (e.g. cell lysate) as they are separated in dynamic isoelectric focusing where fluorescence anisotropy measurement will be performed on separated protein bands to detect a target protein of interest.

Acknowledgment The authors gratefully acknowledge support from National Science Foundation (DBI-0754696 and CHE-0719185). Additional support was provided by Merck & Co., Southern Illinois University at Carbondale and Materials Technology Center.

References

1. Steen J et al (2006) High-throughput protein purification using an automated set-up for high-yield affinity chromatography. Protein Expr Purif 46(2):173–178
2. Yoo MJ, Hage DS (2009) Evaluation of silica monoliths in affinity microcolumns for high-throughput analysis of drug–protein interactions. J Sep Sci 32(15–16):2776–2785
3. Vaya I et al (2010) Drug–protein interactions assessed by fluorescence measurements in the real complexes and in model dyads. Chem Phys Lett 486(4–6):147–153
4. Cuatrecasas P, Wilchek M, Anfinsen CB (1968) Selective enzyme purification by affinity chromatography. Proc Natl Acad Sci U S A 61(2):636–643
5. Jones RB et al (2006) A quantitative protein interaction network for the ErbB receptors using protein microarrays. Nature 439(7073):168–174
6. Cassulis P, Magasic MV, DeBari VA (1991) Ligand affinity chromatographic separation of serum IgG on recombinant protein G-silica. Clin Chem 37(6):882–886
7. Jonker N et al (2008) Screening of protein–ligand interactions using dynamic protein-affinity chromatography solid-phase extraction-liquid chromatography-mass spectrometry. J Chromatogr A 1205(1–2):71–77
8. Kaushansky A et al (2010) Quantifying protein–protein interactions in high throughput using protein domain microarrays. Nat Protoc 5(4):773–790
9. Ahmed FE et al (2010) Surface plasmon resonance (SPR) spectrometry as a tool to analyze nucleic acid–protein interactions in crude cellular extracts. Cancer Genomics Proteomics 7(6):303–309
10. Pan T, Xiao ZD, Huang PM (2009) Characterize the interaction between polyethylenimine and serum albumin using surface plasmon resonance and fluorescence method. J Lumin 129(7):741–745
11. Lamichhane R et al (2010) Single-molecule FRET of protein–nucleic acid and protein–protein complexes: surface passivation and immobilization. Methods 52(2):192–200
12. Ji ZS, Yao ZX, Liu ML (2009) Saturation transfer difference nuclear magnetic resonance study on the specific binding of ligand to protein. Anal Biochem 385(2):380–382
13. Osborne MA (2005) Real-time dipole orientational imaging as a probe of ligand–protein interactions. J Phys Chem B 109(38):18153–18161
14. Barbarakis MS, Bachas LG (1991) Isoelectric focusing electrophoresis of protein–ligand conjugates: effect of the degree of substitution. Clin Chem 37(1):87–90
15. Sreekumar A et al (2001) Profiling of cancer cells using protein microarrays: discovery of novel radiation-regulated proteins. Cancer Res 61(20):7585–7593
16. Stoevesandt O, Taussig MJ, He M (2009) Protein microarrays: high-throughput tools for proteomics. Expert Rev Proteomics 6(2):145–157
17. Montgomery R, Jia X, Tolley L (2006) Dynamic isoelectric focusing for proteomics. Anal Chem 78(18):6511–6518
18. Montgomery R et al (2008) DIABLA: a new screening method for the discovery of protein targets. J Proteome Res 7(10):4594–4597
19. Vaasa A et al (2009) High-affinity bisubstrate probe for fluorescence anisotropy binding/displacement assays with protein kinases PKA and ROCK. Anal Biochem 385(1):85–93

20. Bonarek P et al (2008) Quantitative analysis of the ternary complex of RNA polymerase, cyclic AMP receptor protein and DNA by fluorescence anisotropy measurements. Acta Biochim Pol 55(3):537–547
21. Jameson DM, Ross JA (2010) Fluorescence polarization/anisotropy in diagnostics and imaging. Chem Rev 110(5):2685–2708
22. Valle BC et al (2007) Understanding chiral molecular micellar separations using steady-state fluorescence anisotropy, capillary electrophoresis, and NMR. Langmuir 23(2):425–435
23. Hey T, Lipps G, Krauss G (2001) Binding of XPA and RPA to damaged DNA investigated by fluorescence anisotropy. Biochemistry 40(9):2901–2910
24. Callaway K, Rainey MA, Dalby KN (2005) Quantifying ERK2-protein interactions by fluorescence anisotropy: PEA-15 inhibits ERK2 by blocking the binding of DEJL domains. Biochim Biophys Acta 1754(1–2):316–323
25. Qiao Y et al (2011) Enhanced fluorescence anisotropy assay for human cardiac troponin I and T detection. J Fluoresc 21(6):2101–2110
26. Goltsov A, Lebedeva G, Humphery-Smith I, Goltsov G, Demin O, Goryanin I (2010) In silico screening of nonsteroidal anti-inflammatory drugs and their combined action on prostaglandin H synthase-1. Pharmaceuticals 3:2059–2081
27. Hong Y et al (2008) Population pharmacodynamic modelling of aspirin- and Ibuprofen-induced inhibition of platelet aggregation in healthy subjects. Clin Pharmacokinet 47(2):129–137